Self-reported Surveys

Sensitivity to Punishment and Sensitivity to Reward Questionnaire (SPSRQ). The SPSRQ is a 36-item survey to assess an individual's response to specific cues of punishment and reward (Torrubia et al., 2001; Vandeweghe et al., 2016). Sixteen items measure the sensitivity to reward, and twenty items measure the sensitivity to punishment. This survey is a 5-point Likert-type scale with options ranging from "Never" (score 1) to "Always" (score 5). Higher scores indicate greater sensitivity to punishment and reward.

Behavioral Inhibition System/Behavioral Activation System (BIS/BAS) Scales. The BIS/BAS scales are a 14-item behavioral assessment to measure an individual's reaction to general cues of punishment (BIS) and reward (BAS; (Carver & White, 1994). The BIS scale contains 6 items, e.g., "I feel pretty worried or upset when I think or know somebody is angry at me." For the BAS scale, there are 8 items, e.g., "I go out of my way to get things I want". On a 4-point Likert scale, responses range from "completely disagree" to "completely agree." High scores on the BIS and BAS scale indicate greater sensitivity to punishment and reward cues, separately.

Results for BIS/BAS and SPSRQ. As shown in Table S1, individual sensitivity to reward and punishment was captured by two self-reported questionnaires in Table 3. The results show an average BIS score of 19.42 (SD = 3.28) and a BAS score of 24.61 (SD = 3.84). Additionally, sensitivity to reward has a mean score of 50.74 (SD = 9.32), while sensitivity to punishment averages 60.39 (SD = 12.72) in SPSRQ.

Table S1

Mean and Standard Deviation (SD) of Questionnaires (N=38)

Surveys	Mean	SD
BIS	19.42	3.28
BAS	24.61	3.84
SPSRQ Reward	50.74	9.32
SPSRQ Punishment	60.39	12.72

Note. BIS = Brain Inhibition Scale, BAS = Brain Activation Scale, SPSRQ = Sensitivity to Punishment and Sensitivity to Reward Questionnaire.

Univariate Model for Block Feedback

Univariate Analysis. To model risk features of positive feedback, the contrast between RR and GR positive feedback for BOLD signals was conducted. To model the receipt of reward without risk, we compared GR positive feedback and Neutral feedback. To model the receipt of reward with and without risk, we compared RR and GR positive feedback with Neutral feedback. For loss outcomes, we used the contrast [RR negative > Neutral feedback] for BOLD signals.

Univariate Results. As shown in Table S2, the RR positive > GR contrast yielded greater activation in bilateral occipital regions, right MFG, bilateral posterior MTG, right hippocampus and left ACC. The RR positive > Neutral feedback showed robust BOLD signals in bilateral MFG, right lateral OFC, right PCC, and bilateral occipital cortex. The GR > Neutral feedback coincided with greater BOLD signals in bilateral inferior lateral occipital cortex. Compared with neural feedback, total positive feedback in RR and GR condition coincides with greater brain activation in a large cluster of bilateral lingual gyrus and MFG, right PCC and right dorsolateral inferior frontal gyrus. The RR negative > Neutral feedback coincides with greater BOLD in bilateral inferior and superior lateral occipital cortex and right lingual cortex.

Table S2
Peak Coordinates for Significant Voxels Identified by TFCE

Contrast	Brain Areas	*k*	t-value	X	Y	Z
RR Negative > Neutral Feedback						
	L Lateral Occipital Cortex, inferior division	2240	5.71	-27	-94.5	6
	R Lingual Gyrus	69	5.18	3	-82.5	-1.5
	L Lateral Occipital Cortex, superior division	28	4.22	-33	-85.5	22.5
	R Lateral Occipital Cortex, inferior division	26	4.16	31.5	-84	-3
	R Lateral Occipital cortex, superior division	15	4.34	16.5	-99	7.5
	R Lateral Occipital cortex	11	4.38	12	-99	3
GR Positive> Neutral Feedback						
	L Lateral Occipital Cortex, inferior division	6300	5.39	-33	-87	12
	R Lateral Occipital Cortex, inferior division	5762	8	48	-66	-4.5
RR + GR Positive > Neutral Feedback						

	L Lingual Gyrus	28148	7.29	13.5	-97.5	3
	R middle frontal gyrus	891	6.02	40.5	42	15
	L Middle frontal gyrus	418	5.79	-46.5	45	-9
	R Cingulate Gyrus, posterior division	37	5.48	1.5	-28.5	28.5
	R Cuneal Cortex	29	3.6	4.5	-94.5	33
	L Middle frontal gyrus	23	4.31	-31.5	61.5	12
	R Lateral orbitofrontal cortex	18	4.79	25.5	45	-12
	R Lateral Occipital Cortex, superior division	11	3.39	28.5	-58.5	34.5
	R Superior Frontal Gyrus	10	3.92	31.5	67.5	1.5
RR Positive >Neutral Feedback						
	L Lingual Gyrus	34072	7.94	13.5	-97.5	3
	R Middle Frontal Gyrus	3559	5.67	40.5	40.5	15
	L Middle frontal gyrus	716	6.28	-45	45	-9
	L Paracingulate Gyrus	380	5.79	-1.5	49.5	7.5
	L middle frontal gyrus	88	4.39	-39	61.5	9
	L Cingulate Gyrus, posterior division	83	5.08	1.5	-28.5	28.5
	R Inferior Frontal Gyrus, pars opercularis	48	4.46	57	12	18
	L Frontal Orbital Cortex	40	4.4	-39	19.5	-7.5
	R Frontal Orbital Cortex	27	3.87	45	27	-15
	R Precentral Gyrus	24K67	4.7	43.5	3	27
	R Supramarginal Gyrus, posterior division	18	4.05	43.5	-34.5	33
	R Paracingulate Gyrus	15	4.37	12	46.5	1.5
RR Positive > GR Positive Feedback						
	L Intracalcarine Cortex	10743	5.78	1.5	-46.5	-4.5
	R middle frontal gyrus	2876	5.34	43.5	57	9
	R Middle Temporal Gyrus, posterior division	1043	5.17	51	-25.5	-10.5
	L Cingulate Gyrus, anterior division	745	5.07	-1.5	49.5	7.5
	R Angular Gyrus	432	4.18	52.5	-58.5	33

R Parahippocampal Gyrus, posterior division	247	4.51	16.5	-25.5	-16.5
R Lateral Occipital Cortex, inferior division	66	3.29	40.5	-67.5	-9
L Middle Temporal Gyrus, posterior division	63	4.93	-69	-22.5	-7.5
L Middle Temporal Gyrus, posterior division	27	3.88	-61.5	-25.5	-9
R Lateral Occipital Cortex, superior division	24	4.2	40.5	-61.5	28.5
R Parahippocampal Gyrus, posterior division	15	3.82	12	-37.5	-6
R Hippocampus	13	2.86	18	-19.5	-12
R Parahippocampal Gyrus, anterior division	13	3.53	10.5	-9	-18
R Parahippocampal Gyrus, posterior division	12	3.42	28.5	-28.5	-15

Notes. Whole-brain analyses were conducted at a voxel threshold of $p_{FWE} < 0.05$ by TFCE. $k>10$, parametric modulator = the number of pumps. The local maxima coordinates were included in RR > Neutral Decision contrast. The voxel size is 1.5*1.5*1.5 mm^3 and the total number of voxels is 2,529,432. *Abbreviation*. TFCE, threshold-free clustering enhancement; L, left; R, right; *k*, voxel size.

Comparison between Multi-echo and Single-echo Scanning in RR > GR Decision-making

Univariate Analysis for single-echo Data. To explore differences in sensitivity to BOLD signals between multi-echo and single-echo fMRI for the RR > GR contrast, we repeated the univariate permutation analysis using single-echo EPI images. Specifically, the second-echo EPI images were preprocessed in AFNI following the same steps as for the multi-echo data (Cox & Hyde, 1997). Because only single-echo data were available, tedana denoising was not applied in the entire preprocessing analysis. However, the single-echo partial brain images from the same four participants also failed to co-register with the AFNI preprocessing pipeline. So, FLIRT and ANTs were similarly applied to preprocess their single-echo data (Avants et al., 2009; Woolrich et al., 2009). The preprocessed single-echo data were then applied to the same first- and higher-level analyses in FSL (Woolrich et al., 2009)

Univariate Results for Single-echo Data. The exploratory single-echo analysis produced similar results across cortical regions but was less sensitive to subcortical nuclei. Specifically, the [RR > GR] decision-making contrast coincide with greater BOLD signals in bilateral frontal operculum extending to the orbitofrontal cortex (OFC) and anterior insula (AIC), as well as in the bilateral caudate, left putamen, left nucleus accumbens (NAcc), right middle frontal gyrus (MFG), and brainstem (Table S3). However, the activated frontal-mesolimbic regions (e.g., OFC, AIC and NAcc and dorsal striatum) were smaller than those observed in the multi-echo univariate results (see Figure S1). Further, multi-echo findings, such as activation in VTA and thalamus, were not detected in the single-echo analysis. The comparison between single- and multi-echo univariate results were presented in Figure S1. Results imply that multi-echo imaging offers improved temporal and spatial resolution for investigating subcortical nuclei, compared with traditional single echo imaging as others have argued (Gilmore et al., 2022; Kundu et al., 2012; Steel et al., 2022) .

Table S3

Single-echo Results: Peak Coordinates for TFCE Significantly Activated for Contrasts

Contrast	Brain Areas	Voxels	t	X	Y	Z
RR>NR Decision						
	L Cuneus Cortex	4208	6.35	-7.5	-99	3
	R Middle Frontal Gyrus	1708	7.12	39	55.5	10.5
	R Frontal Operculum Cortex	1053	7.34	40.5	18	3
	L Frontal Operculum Cortex	832	6.4	-40.5	16.5	-1.5
	R Caudate	504	6.35	9	15	7.5

R Inferior Frontal Gyrus, pars opercularis	77	4.62	54	13.5	21
L Caudate	43	5.88	-13.5	16.5	-1.5
R Caudate	29	4.84	16.5	19.5	12
L Caudate	26	4.49	-7.5	3	4.5
R Cerebral White Matter	22	4.14	12	16.5	19.5
R Inferior Frontal Gyrus, pars opercularis,	21	4.71	51	7.5	12
Right Superior Colliculus	16	4.76	3	-33	0

Notes. Whole-brain analyses were conducted at a voxel threshold of pFWE < 0.05 by TFCE. k>10, parametric modulator = the number of pumps. The voxel size is 1.5*1.5*1.5 mm3 and the total number of voxels is 2,529,432. Abbreviation. TFCE, threshold-free clustering enhancement; L, left; R, right; k, voxel size.

Figure S1

TFCE-corrected t-value Map for single-echo images

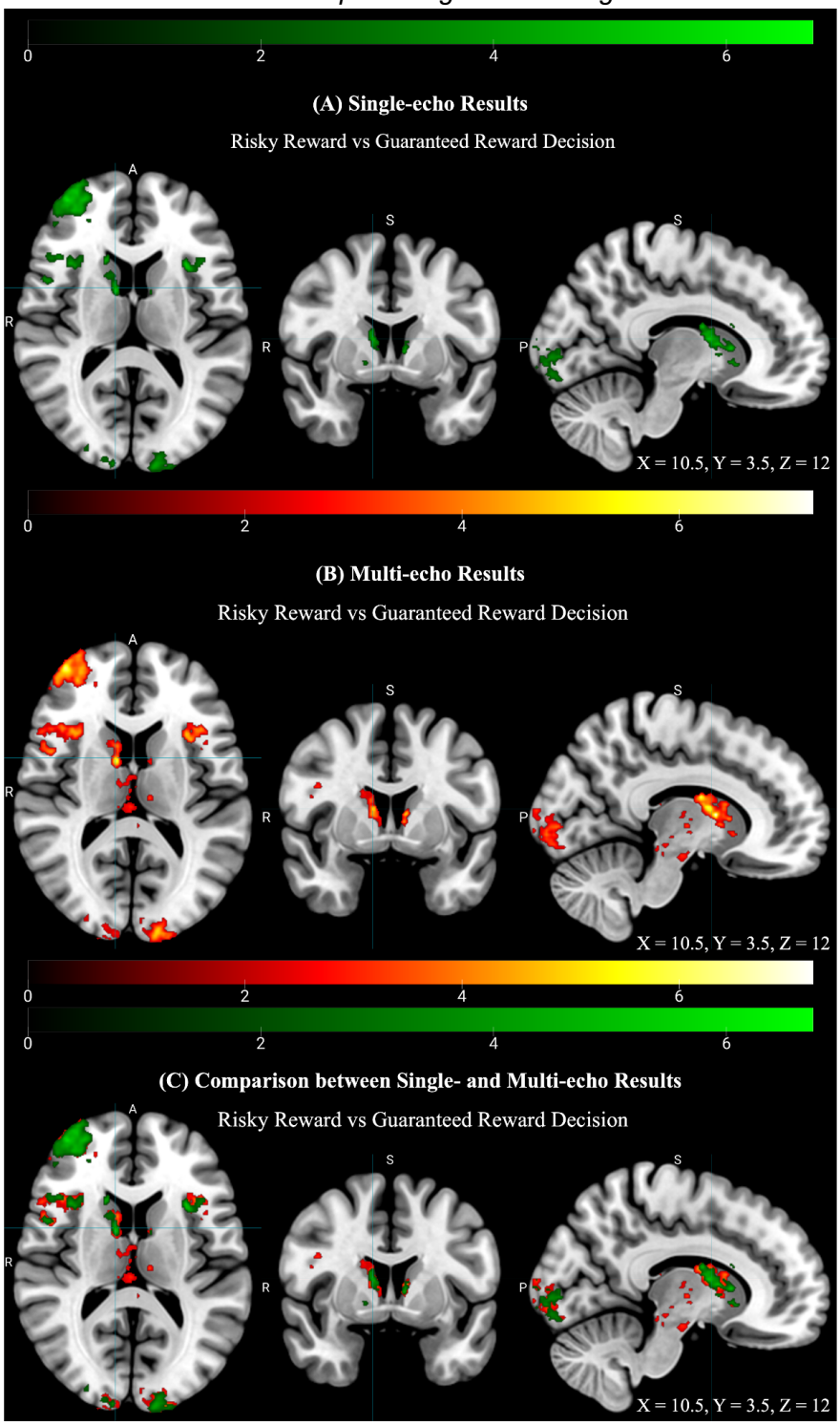

Reference

Avants, B., Tustison, N. J., & Song, G. (2009). Advanced Normalization Tools: V1.0. *The Insight Journal*. https://doi.org/10.54294/uvnhin

Carver, C. S., & White, T. L. (1994). Behavioral inhibition, behavioral activation, and affective responses to impending reward and punishment: The BIS/BAS Scales. *Journal of Personality and Social Psychology*, *67*(2), 319–333. https://doi.org/10.1037/0022-3514.67.2.319

Cox, R. W., & Hyde, J. S. (1997). Software tools for analysis and visualization of fMRI data. *NMR in Biomedicine*, *10*(4–5), 171–178. https://doi.org/10.1002/(sici)1099-1492(199706/08)10:4/5<171::aid-nbm453>3.0.co;2-l

Gilmore, A. W., Agron, A. M., González-Araya, E. I., Gotts, S. J., & Martin, A. (2022). A Comparison of Single- and Multi-Echo Processing of Functional MRI Data During Overt Autobiographical Recall. *Frontiers in Neuroscience*, *16*. https://doi.org/10.3389/fnins.2022.854387

Kundu, P., Inati, S. J., Evans, J. W., Luh, W.-M., & Bandettini, P. A. (2012). Differentiating BOLD and non-BOLD signals in fMRI time series using multi-echo EPI. *NeuroImage*, *60*(3), 1759–1770. https://doi.org/10.1016/j.neuroimage.2011.12.028

Steel, A., Garcia, B. D., Silson, E. H., & Robertson, C. E. (2022). Evaluating the efficacy of multi-echo ICA denoising on model-based fMRI. *NeuroImage*, *264*, 119723. https://doi.org/10.1016/j.neuroimage.2022.119723

Torrubia, R., Ávila, C., Moltó, J., & Caseras, X. (2001). The Sensitivity to Punishment and Sensitivity to Reward Questionnaire (SPSRQ) as a measure of Gray's anxiety and impulsivity dimensions. *Personality and Individual Differences*, *31*(6), 837–862. https://doi.org/10.1016/S0191-8869(00)00183-5

Vandeweghe, L., Matton, A., Beyers, W., Vervaet, M., Braet, C., & Goossens, L. (2016).

Psychometric properties of the BIS/BAS Scales and the SPSRQ in Flemish adolescents. *Psychologica Belgica*, *56*(4), 406. https://doi.org/10.5334/pb.298

Woolrich, M. W., Jbabdi, S., Patenaude, B., Chappell, M., Makni, S., Behrens, T., Beckmann, C., Jenkinson, M., & Smith, S. M. (2009). Bayesian analysis of neuroimaging data in FSL. *NeuroImage*, *45*(1), S173–S186. https://doi.org/10.1016/j.neuroimage.2008.10.055